Anuário do Instituto de Geociências
Universidade Federal do Rio de Janeiro
https://revistas.ufrj.br/index.php/aigeo/

ISSN 0101-9759
e-ISSN 1982-3908

Permeability Data Treatment from Analogous Outcrop for use in Three-Dimensional Reservoir Model

Tratamento de Dados de Permeabilidade de Afloramento Análogo para uso em Modelo Tridimensional de Reservatórios

Camila Faria de Albuquerque[1], Aline Theophilo Silva[1] & Claudio Limeira Mello[2]

[1]Centro de Pesquisas, Desenvolvimento e Inovação Leopoldo Américo Miguez de Mello – PETROBRAS, Rio de Janeiro, RJ, Brasil
[2]Universidade Federal do Rio de Janeiro Departamento de Geologia, Instituto de Geociências, Rio de Janeiro, RJ, Brasil

E-mails: camilafaria@petrobras.com.br; alinet@petrobras.com.br; limeira@geologia.ufrj.br
Corresponding author: Camila Faria de Albuquerque; camilafaria@petrobras.com.br

Abstract

Over the past forty years, the study of analogous outcrops has become a common practice in the petroleum industry to access more comprehensive geological datasets and better parameterize various geological features. As most reservoirs do not outcrop and all the data obtained are restricted to those collected from wells located in areas of major interest or from indirect measurements, the study of analogous outcrops has brought important contributions to improve the production routines and still represents a helpful information resource. The use of data from analogous outcrops permits, for example, to estimate the sedimentary facies distribution in true reservoirs, and thus to improve on the reliability of fluid flow modeling during the oil field exploration. However, such data must be processed to become equivalent to the data collected under the reservoir conditions and the results obtained to be more realistic. This work presents the statistical method used to make permeability data obtained from an outcrop compatible with the subsurface conditions of poorly consolidated and tectonically deformed sandstone reservoirs. The studied outcrop is predominantly composed of Eocene fluvial sandstones (Resende Formation) of the Volta Redonda Basin, located in the Central Segment of the Continental Rift of Southeastern Brazil. These deposits are affected by deformation bands and faults. From statistical analysis, it was intended that the permeability data become more suitable to be used, in the next phase of the studies, to build a 3D flow model, in which it will be possible to test the potential of different tectonic structures acting as hydraulic barriers in poorly consolidated and deformed reservoirs. The methodological approach applied in this study made it possible to turn compatible the permeability data obtained in conditions of no confining pressures from the outcrop with reservoir conditions under confinement pressures of 2,000 psi. Such pressure conditions are frequently observed in important Maastrichtian reservoirs found in the Brazilian Southeastern Margin.

Keywords: Poorly consolidated sandstones; Reservoir properties modeling; Statistical analysis.

Resumo

O estudo de afloramentos análogos tornou-se, nos últimos quarenta anos, uma prática comum na indústria petrolífera, possibilitando a obtenção de conjuntos de dados geológicos mais abrangentes e a melhor parametrização de diversos aspectos geológicos. Como a maioria dos reservatórios não aflora e todos os dados obtidos se restringem àqueles coletados em poços localizados em áreas de maior interesse ou por meio de medições indiretas, o estudo de afloramentos análogos trouxe contribuições importantes para melhorar as rotinas de produção, ainda representando um recurso útil de informação. O uso de dados de afloramentos análogos permite, por exemplo, estimar a distribuição de fácies sedimentares em reservatórios reais e, assim, melhorar a confiabilidade da modelagem de fluxo de fluidos durante a exploração de campos petrolíferos. Entretanto, tais dados devem ser processados para que se tornem equivalentes aos dados coletados nas condições do reservatório e os resultados obtidos sejam mais realistas. Este trabalho apresenta o método estatístico utilizado para tornar dados de permeabilidade obtidos em um afloramento compatíveis com as condições em subsuperfície de reservatórios areníticos pouco consolidados e tectonicamente deformados. O afloramento estudado é composto predominantemente por arenitos fluviais eocênicos (Formação Resende) da Bacia de Volta Redonda, localizada no Segmento Central do *Rift* Continental do Sudeste do Brasil. Esses depósitos são afetados por bandas de deformação e falhas. A partir do tratamento estatístico, pretendeu-se que os dados de permeabilidade se tornassem mais adequados para serem utilizados, em uma próxima etapa dos estudos, na construção de

Received: 15 June 2023; Accepted: 17 December 2023

um modelo de fluxo 3D, no qual será possível testar o potencial de diferentes estruturas tectônicas atuando como barreiras hidráulicas em reservatórios pouco consolidados e deformados. A abordagem metodológica aplicada neste estudo possibilitou compatibilizar os dados de permeabilidade obtidos em condições de não confinamento do afloramento com condições de reservatório sob pressões de confinamento de 2.000 psi. Tais condições de pressão são frequentemente observadas em importantes reservatórios maastrichtianos encontrados na Margem Sudeste do Brasil.

Palavras-chave: Arenitos pouco consolidados; Modelagem de propriedades de reservatório; Análises estatísticas

1 Introduction

Modeling the petrophysics properties of oil reservoirs is one of the key stages for a successful production decision tree since those models allow better selection of the position of new wells, getting more efficient strategies to enhance the production rates, and to plain the best logistics of all production equipment installation. Direct data, like sidewall samples and well-core samples, have high costs and low accuracy due to the lithological and structural variability usually found in natural geological conditions. So, a practice frequently used by the industry to improve the efficiency of reservoir simulation predictions is the study of analogous outcrops. This type of study makes it possible to acquire a significant amount of information from specific geological aspects equivalent to those found in subsurface reservoirs, directly and with lower costs. This approach favors the establishment of the three-dimensional sedimentary facies distribution and their relationships in the depositional system, and the tectonic structures framework on subseismic scales (Howell, Martinius & Good 2014).

The use of analogous outcrops also helps to understand the relationship between rocks and their porosity and permeability properties. However, these parameters may suffer significant value variations when the rocks are submitted to subsurface confining pressures, or when the outcrops are under unconfined pressure conditions. When rocks are buried, the porosity and permeability values tend to decrease due to the material compaction, whereas when the rocks are at the surface, or near it, these properties are closer to the original values. Concerning this question, it becomes essential to evaluate how measurements obtained in outcrops can be used in a geological reservoir model.

In this study, we present a proposal for a method to turn compatible the permeability values obtained in an outcrop to the permeability values at a confined pressure equivalent to Maastrichtian reservoir found in the Southeastern Brazilian marginal basin, estimated at 2,000 psi.

2 Geological Setting

The outcrop investigated in this study is in the Volta Redonda Basin (Figure 1), which is the smallest of the Cenozoic basins in the Central Segment of the Continental Rift of Southeastern Brazil (Negrão et al. 2015; Negrão et al. 2020; Riccomini, Sant'anna & Ferrari 2004; Sanson 2006).

According to Negrão et al. (2020), the main stratigraphic unit of the Volta Redonda Basin is the Resende Formation (Eocene), which is composed of lenticular to tabular intervals of poorly consolidated stratified feldspathic sandstones, interbedded with fine conglomerates and greenish mudstones. These deposits are related to the sedimentation in braided rivers and alluvial fans during the rift formation. Alkaline ultrabasic volcanic rocks (Casa de Pedra Basanite) are also associated with the rift phase. Oligocene braided fluvial deposits form the Pinheiral Formation, in an erosive contact over the Resende Formation e Casa de Pedra Basanite. Above the Paleogene units, there are Quaternary colluvial and alluvial deposits.

The Volta Redonda Basin evolved in the context of the Continental Rift of Southeastern Brazil (RCSB – Riccomini 1989; Riccomini et al. 2004), in which five tectonics events are identified: Paleogene NW-SE extension (E1) – rift phase; Miocene E-W sinistral strike-slip event (ST); Pleistocene E-W dextral strike-slip event (DT); Holocene NW-SE extension (E2); and the modern E-W compression (C).

The studied outcrop is approximately 18 m high and 54 m long, and it is subdivided into two slopes (lower and upper) separated by a berm (Figure 2). The outcrop is predominantly composed of deposits of the Resende Formation. At the upper part of the outcrop, there is a small and quite weathered exposure of Pinheiral Formation deposits. Two normal faults ("F1" and "F2") with ENE-WSW orientation and opposite dips split the outcrop into three main sectors (north, central, and south – Maciel, Mello & Silva 2017). Other secondary faults also occur through the outcrop and deformation band zones are concentrated at the south sector. The main faults and the deformation band zones are associated with the strike-slip events and were reactivated during the E2 event; and the secondary faults present in the central sector are related to the E2 event (Fiuza, Mello & Ribeiro 2020; Maciel, Mello & Silva 2017).

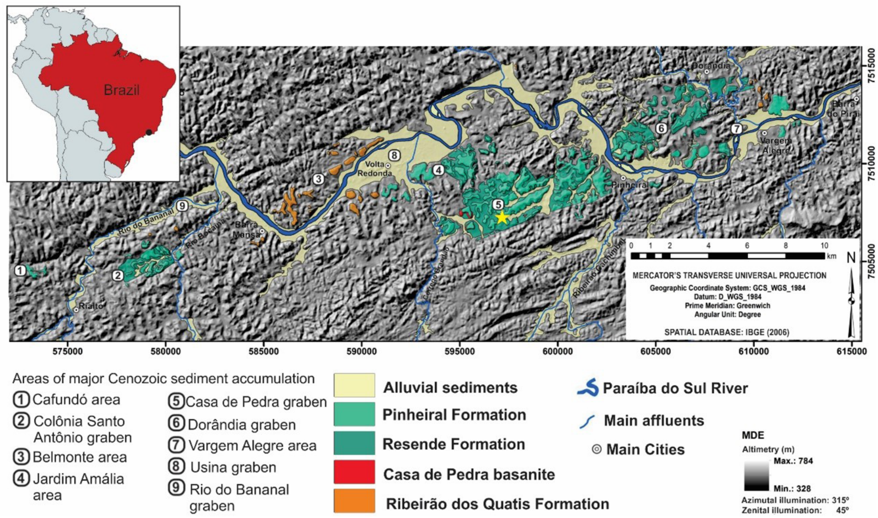

Figure 1 Map of the Cenozoic sedimentary units of the Volta Redonda Basin over the relief shading model, emphasizing the strong control of the distribution of Paleogene deposits by NE-SW structures and, subordinately, NW-SE structures. The yellow star indicates the location of the studied outcrop. Modified from Negrão et al. (2015).

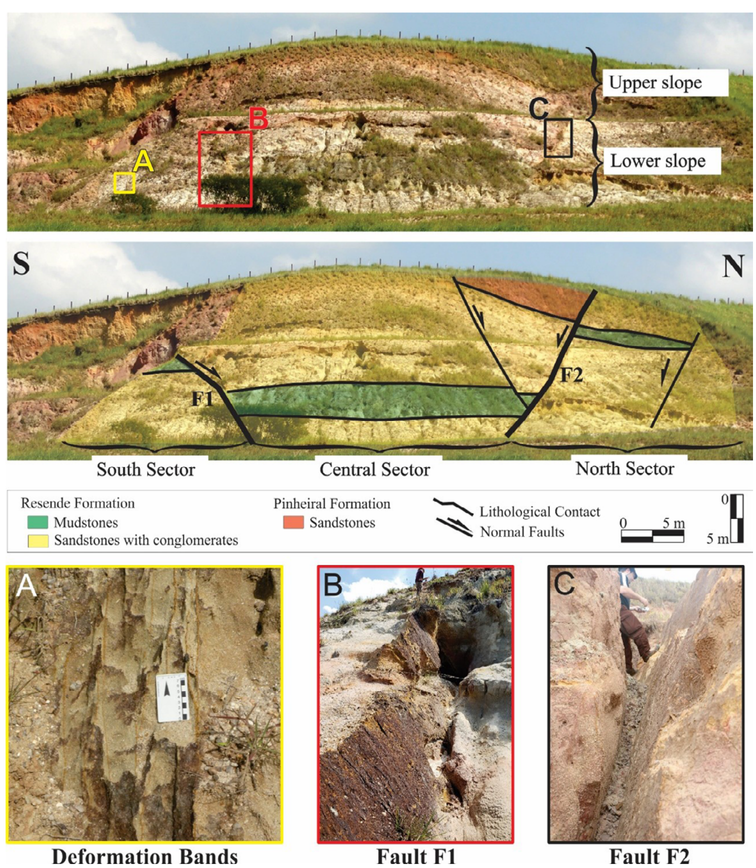

Figure 2 General aspects of the studied outcrop, showing the main lithologic contacts and the major tectonic structures: **A.** Deformation bands in the south sector; **B.** Ferruginized plane of Fault F1; **C.** Clay smear on Fault F2.

3 Materials and Methods

The main dataset analyzed in the present study comprises more than 5,000 in-situ permeability measurements collected by Galvão (2018) and Andrade (2020) on the studied outcrop using a TinyPerm3 mini-permeameter. These data include permeability measurements in three orthogonal directions (two horizontal and one vertical). Horizontal readings were obtained parallel and perpendicular to the main faults (F1 and F2). Data acquisition was guided by a regular 2x2 m grid along the outcrop, which also served as the basis for the representation of the sedimentary layers and tectonic structures (deformation bands and faults) in a geological section at a scale of 1:50 (Mello et al. 2021; Figure 3). Galvão (2018) and Andrade (2020) collected more than 10 permeability readings in each orthogonal direction by each cell grid to guarantee the best accuracy of the mean value calculated for each direction.

Another dataset here analyzed corresponds to porosity and permeability measurements obtained in the laboratory. These measurements were carried out by Galvão (2018), Vogel (2018), and Mello et al. (2021) from plugs extracted from the rock blocks collected at the outcrop.

The in-situ permeability values from previous studies (Galvão 2018; Andrade 2020) needed to be statistically processed to adjust the results from the unconfined pressure conditions to the confined pressure found in reservoir conditions.

The first stage of the statistical processing (Figure 4) was the calculation of the geometric mean for each permeability direction (i.e., vertical, parallel, and perpendicular) on each cell grid (Table 1). The geometric mean was adopted because it is the calculation modality most used in the petroleum industry, applied in cases where permeability changes smoothly (Liao 2018).

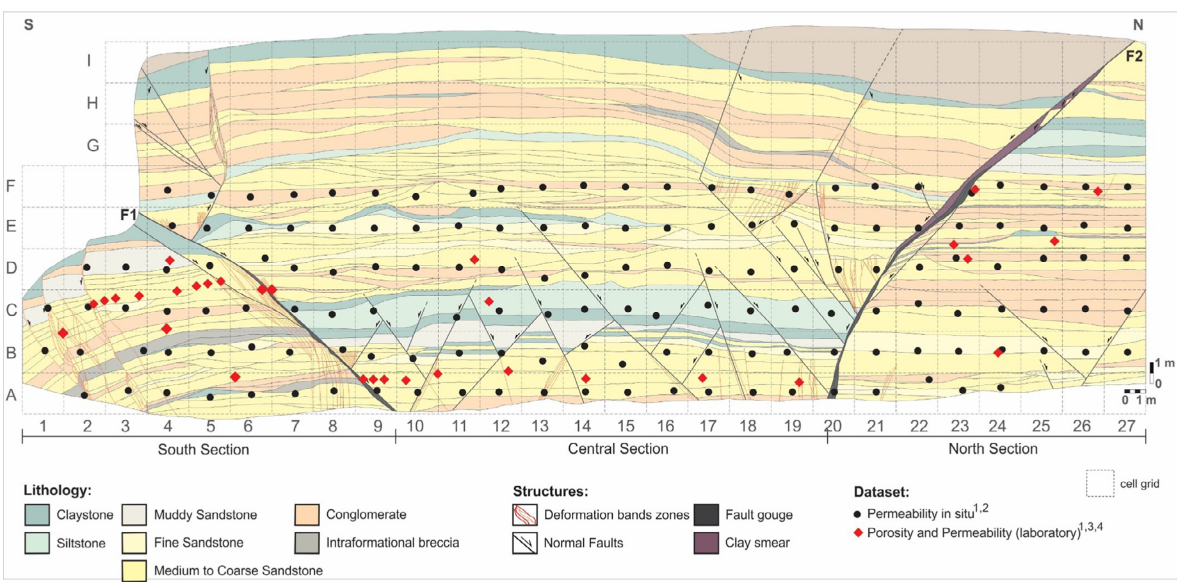

Figure 3 Localization of porosity and permeability data in the studied outcrop. Samples were collected only on the lower slope of the outcrop.

Data collected by (1) Galvão (2018); (2) Andrade (2020); (3) Vogel (2018); (4) Mello et al. (2021).

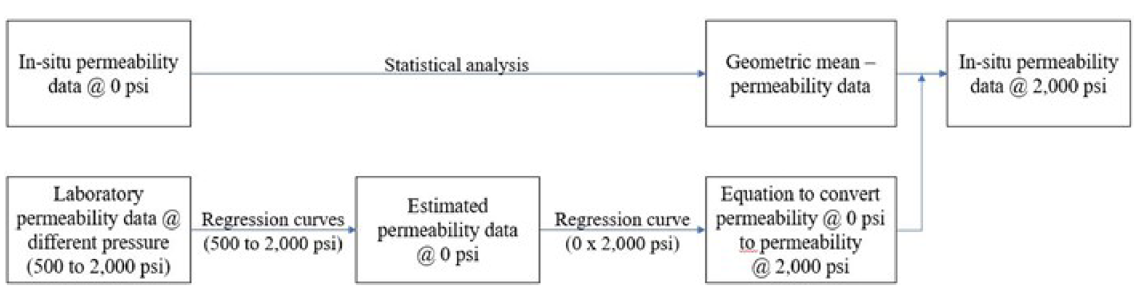

Figure 4 Methodological stages.

Table 1 Example of the permeability readings (cell grid A02) for each orthogonal direction and the averages obtained to represent it.

Lithology	Cell Grid	Vertical Permeability (mD)	Parallel Permeability (mD)	Perpendicular Permeability (mD)
Medium to Coarse Sandstone	A02	33,678.66	63,232.27	29,904.86
		56,279.23	64,132.51	55,585.91
		36,192.25	49,476.92	48,752.20
		35,805.79	63,345.48	23,899.55
		51,567.42	69,900.05	25,950.67
		49,235.13	59,361.18	39,614.31
		32,429.76	61,964.13	31,707.01
		88,856.43	47,157.03	67,226.60
		58,313.76	76,732.06	64,336.04
		68,978.98	52,991.88	66,275.02
		-	-	37,456.77
		-	-	49,201.80
Median		50,401.27	62,598.20	44,183.25
Arithmetic mean		51,133.74	60,829.35	44,992.56
Geometric mean		**48,518.15**	**60,214.19**	**42,357.01**
Harmonic mean		46,198.30	59,593.06	39,783.97

The next step was to transform the geometric mean values to pressure conditions equivalent to 2,000 psi. For this, regression curves were made using the permeability data acquired in the laboratory by Galvão (2018) and Mello et al. (2021) for a set of samples submitted to different confinement pressures (500; 1,000; 1,500; 2,000 psi; Table 2) to achieve an estimated permeability at 0 psi. Following, a new regression curve was built using the estimated permeability values at 0 psi in relation to the permeability values at 2,000 psi, for each sample. The resulting equation was applied to the geometric mean values at 0 psi permeability dataset to obtain the geometric mean values at 2,000 psi.

4 Results

The geometric mean values of the in-situ permeability data collected by Andrade (2020) for different lithologies allow to classify them into reservoir facies, considering their order of magnitude variability (Table 3). This way, claystone and siltstone can be grouped as non-reservoir, fine sandstone and muddy sandstone as poor reservoir, and medium to coarse sandstone, conglomerate and intraformational breccia as good reservoir. The geometric mean values of the in-situ measurements done for each cell grid are presented in Figure 5. The geometric mean for each reservoir facies versus the dispersion of the in-situ permeability values is shown in Figure 6.

The regression curves obtained to estimate the in-situ permeability at 0 psi using the permeability values of the samples analyzed in the laboratory at different confining pressures (500, 1,000, 1,500 and 2,000 psi – Figure 7) show coefficient of determination values greater than 0.92, indicating that the models have an excellent fit, as presented in Table 4. The values estimated at 0 psi with the regression curve for each sample showed results with the same order of magnitude as the geometric mean of the in situ permeability measurements obtained by Andrade (2020) in each corresponding cell grid.

The regression function obtained from the correlation between the measured permeability values at a confinement pressure of 2,000 psi and the estimated permeability values at 0 psi for all samples (Equation 1) presented a coefficient of determination (R^2) equal to 0,7985 (Figure 8). Although this coefficient of determination is lower than the ones obtained in the previous methodological step, it still presents good reliability to be applied for the conversion of the in-situ permeability dataset to the confined permeability at 2,000 psi.

$$Perm_{2000\ psi} = 0.2872 \times \left(Perm_{0\ psi}\right)^{1.0343} \qquad (1)$$

Table 2 Permeability values of the laboratory samples at different confining pressures (500, 1,000, 1,500, and 2,000 psi) (Galvão 2018; Mello et al. 2021). MCS: Medium to Coarse Sandstone, FS: Fine Sandstone, Co: Conglomerate, MS: Muddy Sandstone, Si: Siltstone.

Sample	Lithology analyzed	Laboratory permeability (mD) – confining pressure			
		500 psi	1,000 psi	1,500 psi	2,000 psi
26 (BA-0)	MCS	1,760	1,470	1,310	894
20 (BB-1)	MCS	268	220	180	138
39 (BB-3)	MCS	531	505	419	293
30 (BB-5)	MCS	662	565	436	334
1-24B	FS	77	41.9	35.1	29
2-23D	Co	8,430	4,260	2,540	2,120
3-4D	MS	142	119	99.8	79.3
5-11D	MCS	2,070	1,700	1,420	1,150
6-12C	Si	21.4	15.1	8.71	4.8
7-19A	MCS	620	470	375	333
8-14A	MCS	1,380	1,260	1,060	853

Table 3 Geometric mean values of the permeabilities at 0 psi separated by lithology.

	Geometric mean permeability values @ 0 psi (mD)		
	Perpendicular	Parallel	Vertical
Claystone	16	41	14
Siltstone	18	8	7
Fine Sandstone	336	183	142
Muddy Sandstone	533	526	597
Medium to coarse sandstone	2,377	1,693	1,994
Conglomerate	7,842	6,928	6,378
Intraformational Breccia	8,987	2,918	399

Green: Non-reservoir; Red: Poor reservoir; Yellow: Good reservoir

Perpendicular Permeability (mD) @ without confining pressure

	1	2	3	4	5	6	7	8	9	10	11	12	13	14	15	16	17	18	19	20	21	22	23	24	25	26	27
F				15019	195	2289	576	3625	717	1907	3870	3821	24807	6424	2707	12128	2205	465	1930	1361	4094	30289	15061	13598	13816	13507	12332
E				4437	5.8	1.2	26112	828	319	833	278	1.2	1137	2992	1791	4170	7719	12136	2148	1414	1217	15	19343	10446	22754	27532	18829
D		437	691	1000	228	372	1895	1197	1132	6202	1259	1294	6532	368	68	1053	95837	2793	892	17	769	77695	38253	86750	12361	170824	35320
C	256	299	12277	22170	39391	13693	3.5	0.9	3.0		10	33	25	13	69	56	30	76	156	134	1520	36034	133	42404	47655	73117	125573
B	6540	22113	8987	399	19842	6122	11063	26624	3.0	104	11	334	3901	3.6	4498	12	552	526	6.2	5.4	104	46	132	80	105	168	55
A		42357	7894	3404	60842	20530	3867	6443	935	709	12297	4192	9225	12058	16260	15439	15485	5046	677	478	661	905	183	98			

Parallel Permeability (mD) @ without confining pressure

	1	2	3	4	5	6	7	8	9	10	11	12	13	14	15	16	17	18	19	20	21	22	23	24	25	26	27
F				14524	468	1700	326	14831	200	542	1918	2894	11412	7588	1584	4521	2938	21	627	1707	841	23632	16345	10623	15311	8737	9138
E				6030	12	1.1	18444	1178	588	973	413	0.6	523	953	857	799	2604	12411	911	2355	2879	4.4	22694	9252	48574	14735	21087
D		583	456	434	354	218	110	941	197	9306	3119	244	13	38	1197	1735	31855	1139	7.1	46	239	94134	21615	92710	20473	130140	50547
C	121	469	10703	17618	28362	7834	3.5	0.7	1.0		81	3.9	74	1.1	400	110	44	29	19	33	3286	29502	214	59024	69734	89277	83499
B	4150	19811	2918	3773	21324	4857	14701	20710	9.4	7.5	123	6.2	5935	1.4	8957	10	441	462	21	3.7	49	5.2	79	51	735	263	29
A		60214	1094	1851	61743	21979	9818	2115	472	1481	20064	5531	8305	10409	9152	13391	14083	3606	406	142	45	1141	4.9	40			

Vertical Permeability (mD) @ without confining pressure

	1	2	3	4	5	6	7	8	9	10	11	12	13	14	15	16	17	18	19	20	21	22	23	24	25	26	27
F				4630	67	4231	90	2307	1255	1538	5893	6796	25589	8930	2701	15164	1283	106	345	2860	429	55893	16729	10853	13447	7700	9339
E				7427	17	0.7	1130	282	252	423	228	0.8	1117	1364	570	2174	7247	14607	1690	2776	4348	19	21108	4248	49841	13288	27147
D		1167	306	330	74	716	325	452	369	13091	2599	471	916	150	1417	636	24322	1784	20	38	1107	33672	26373	81402	8177	63206	46160
C	41	952	15350	8316	12813	9645	8.6	1.3	0.9		1.3	33	65	66	1.3	46	6.3	6.5	161	45	6128	95091	42	93043	76354	83229	63106
B	4850	24969	399	4519	18964	5784	16795	15344	1.7	15	3.9	13	3082	0.4	3172	95	485	1045	16	11	36	49	114	32	120	100	14
A		48518	956	1714	76652	11312	3540	5951	1282	1000	11984	4421	18104	17261	13193	19935	20456	3758	1403	66	6.9	551	1.1	272			

Non reservoir | Poor reservoir | Good reservoir

Figure 5 Geometric mean values of the permeability raw data collected by Andrade (2020) for each cell grid, according to Figure 3.

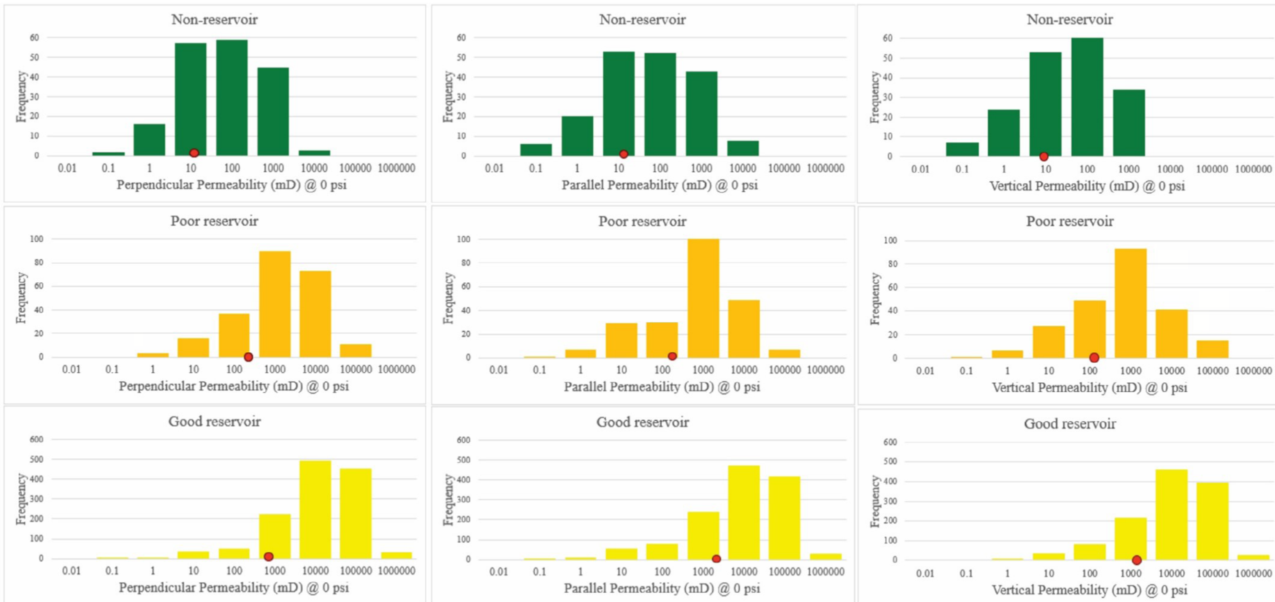

Figure 6 Frequency histogram for each permeability direction at 0 psi, grouped by reservoir facies. The red dot represents the geometric mean for each reservoir facies.

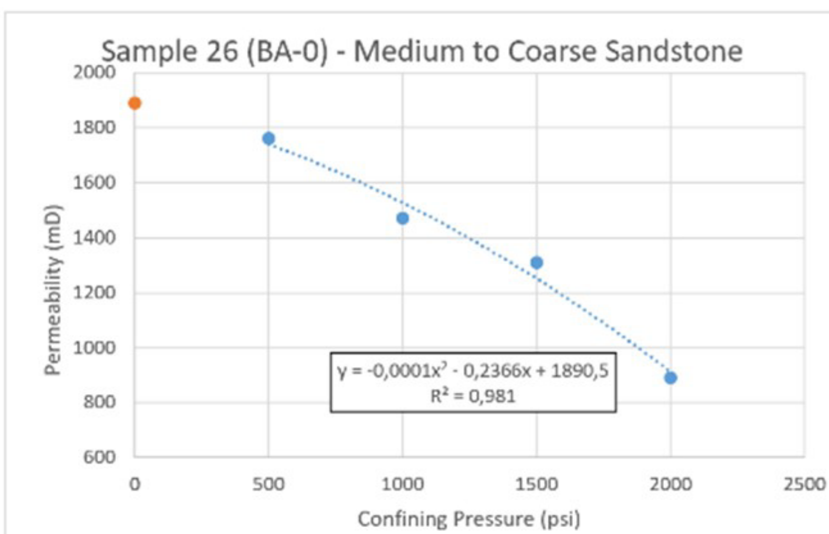

Figure 7 Example of the regression curve used to estimate the in-situ permeability at 0 psi using the permeability data analyzed in the laboratory at different confining pressures. These graphs were done for the 11 samples listed in Table 2.

Table 4 Estimated permeability values at 0 psi after applying the respective regression function for each sample analyzed.

Sample	Lithology analyzed	Laboratory permeability (mD) – confining pressure	Regression function y = permeability x = confining pressure	R^2	Estimated permeability (mD)
		2,000 psi			0 psi
26 (BA-0)	MCS	894	y = – 0,0001x² – 0.2366x + 1890.5	0.981	1,891
20 (BB-1)	MCS	138	y = – 0,000001x² – 0.101x + 316.5	0.9995	317
39 (BB-3)	MCS	293	y = – 0.16x + 637	0.927	637
30 (BB-5)	MCS	334	y = – 0,00005x² – 0.2101x + 771.25	0.9972	771
1-24B	FS	29	y = – 0,00003x² – 0.1027x + 119.7	0.9725	120
2-23D	Co	2,120	y = – 0,0038x² – 13.505x + 14188	0.9973	14,188
3-4D	MS	79.3	y = – 0,000003x² – 0.0477x + 164.98	0.9994	165
5-11D	MCS	1,150	y = – 0,0001x² – 0.858x + 2470	0.9993	2,470
6-12C	Si	4.8	y = – 0,000002x² – 0.0172x + 29.538	0.9979	29.5
7-19A	MCS	333	y = – 0,0001x² – 0.4612x + 823.5	1.00	824
8-14A	MCS	853	y = – 0,00009x² – 0.1387x + 1474.8	0.9983	1,475

MCS (medium to coarse sandstone), FS (fine sandstone), Co (conglomerate), MS (Muddy Sandstone), Si (siltstone).

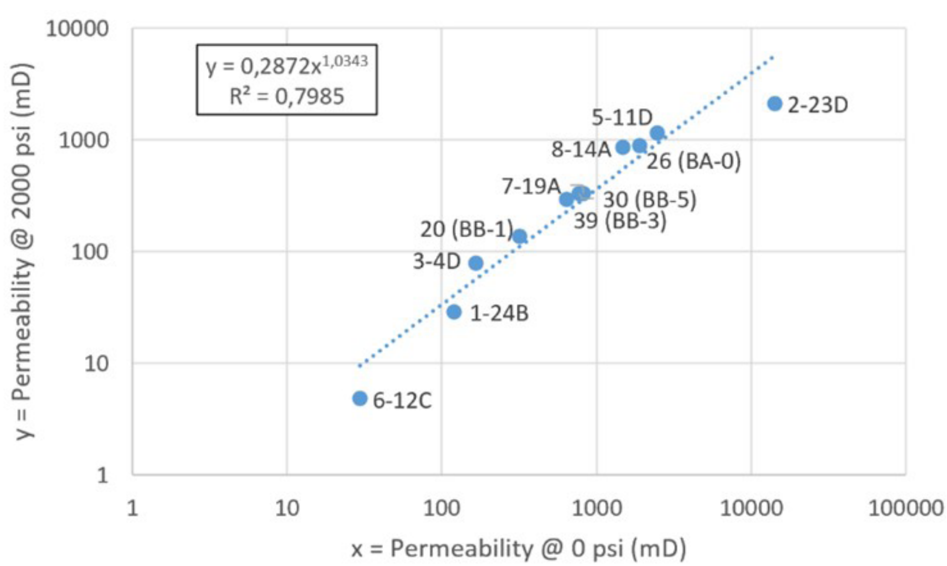

Figure 8 Estimated permeability at 0 psi versus measured permeability at 2,000 psi based on the samples presented in Table 4.

Considering this reliability, Equation 1 was applied to convert the geometric mean permeability values at 0 psi (Figure 5) to geometric mean permeability values at 2,000 psi, as presented in Figure 9. Analyzing the dataset obtained it is possible to observe that the permeability values have a 25-39% loss when adjusted from 0 to 2,000 psi, reducing the order of the magnitude as expected (Figure 10, Table 5). The lowest reduction in permeability values was observed in the non-reservoir lithologies but with higher variability (25-33%). The poor and good reservoir facies showed a major reduction in permeability values with minor variability (34-39%). It is observed that there is a subtle change in the distribution of the pattern of the permeability values, which can be attributed to the change in the threshold values of each class in the histogram.

Perpendicular Permeability (mD) @ 2.000 psi																											
	1	2	3	4	5	6	7	8	9	10	11	12	13	14	15	16	17	18	19	20	21	22	23	24	25	26	27
F				5999	67	857	206	1379	258	709	1475	1456	10081	2492	1019	4809	825	165	719	501	1564	12393	6016	5413	5503	5375	4893
E				1700	1.8	0.4	10630	299	112	301	97	0.4	416	1131	665	1594	3014	4812	803	521	446	4.7	7794	4121	9219	11228	7579
D		154	248	364	79	131	705	438	414	2403	462	475	2536	129	22	384	40793	1053	324	5.5	277	32834	15777	36799	4905	74167	14528
C	89	105	4870	8974	16263	5452	1.0	0.3	0.9		3.2	11	8.1	4.0	23	18	10	25	53	46	561	14832	45	17551	19804	30835	53948
B	2539	8951	3527	141	8002	2371	4373	10845	0.9	35	3.3	117	1488	1.1	1724	3.8	197	187	1.9	1.7	35	15	45	27	36	58	18
A		17531	3084	1292	25497	8289	1474	2500	340	255	4878	1603	3624	4780	6512	6173	6191	1941	243	170	237	328	63	33			

Parallel Permeability (mD) @ 2.000 psi																											
	1	2	3	4	5	6	7	8	9	10	11	12	13	14	15	16	17	18	19	20	21	22	23	24	25	26	27
F				5795	166	630	114	5922	69	193	714	1092	4516	2961	586	1733	1110	6.8	224	633	304	9587	6548	4193	6120	3425	3588
E				2334	3.7	0.3	7419	431	210	354	146	0.2	186	346	310	289	980	4925	331	883	1087	1.3	9194	3635	20199	5882	8521
D		208	162	153	124	75	37	342	68	3657	1180	85	4.1	13	438	643	13056	417	2.2	15	83	40044	8742	39417	8265	55978	21048
C	41	166	4226	7076	11578	3060	1.0	0.2	0.3		27	1.2	25	0.3	141	37	14	9.3	6.0	11	1246	12060	74	24709	29360	37908	35374
B	1586	7989	1102	1437	8621	1866	5868	8364	2.9	2.3	42	1.9	2296	0.4	3515	3.2	156	164	6.7	1.1	16	1.6	26	17	265	91	9.5
A		25225	399	688	25888	8894	3865	790	168	546	8094	2135	3250	4106	3594	5328	5613	1371	143	48	15	417	1.5	13			

Vertical Permeability (mD) @ 2.000 psi																											
	1	2	3	4	5	6	7	8	9	10	11	12	13	14	15	16	17	18	19	20	21	22	23	24	25	26	27
F				1776	22	1618	30	864	460	568	2280	2642	10410	3504	1017	6059	471	36	121	1079	152	23355	6707	4287	5351	3006	3670
E				2896	5.4	0.2	413	98	87	150	79	0.2	408	502	203	813	2823	5829	626	1046	1664	6.0	8530	1625	20744	5286	11066
D		427	107	115	25	258	114	160	130	5204	978	167	332	51	522	228	9877	662	6.4	12	405	13827	10740	34455	3199	26522	19162
C	13	346	6136	3255	5090	3794	2.7	0.4	0.3		0.4	11	22	22	0.4	15	1.9	2.0	55	15	2374	40465	14	39563	32247	35256	26479
B	1864	10149	141	1732	7635	2236	6734	6133	0	4.6	1.2	4.0	1166	0.1	1201	32	172	381	5.2	3.5	12	16	38	10	41	34	4.3
A		20175	347	636	32378	4475	1346	2303	471	364	4750	1693	7278	6928	5246	8040	8258	1431	517	22	2.1	196	0.3	95			

Non reservoir | Poor reservoir | Good reservoir

Figure 9 Geometric mean values of the permeability raw data collected by Andrade (2020) for each cell grid, according to Figure 3, converted to confinement pressure at 2,000 psi.

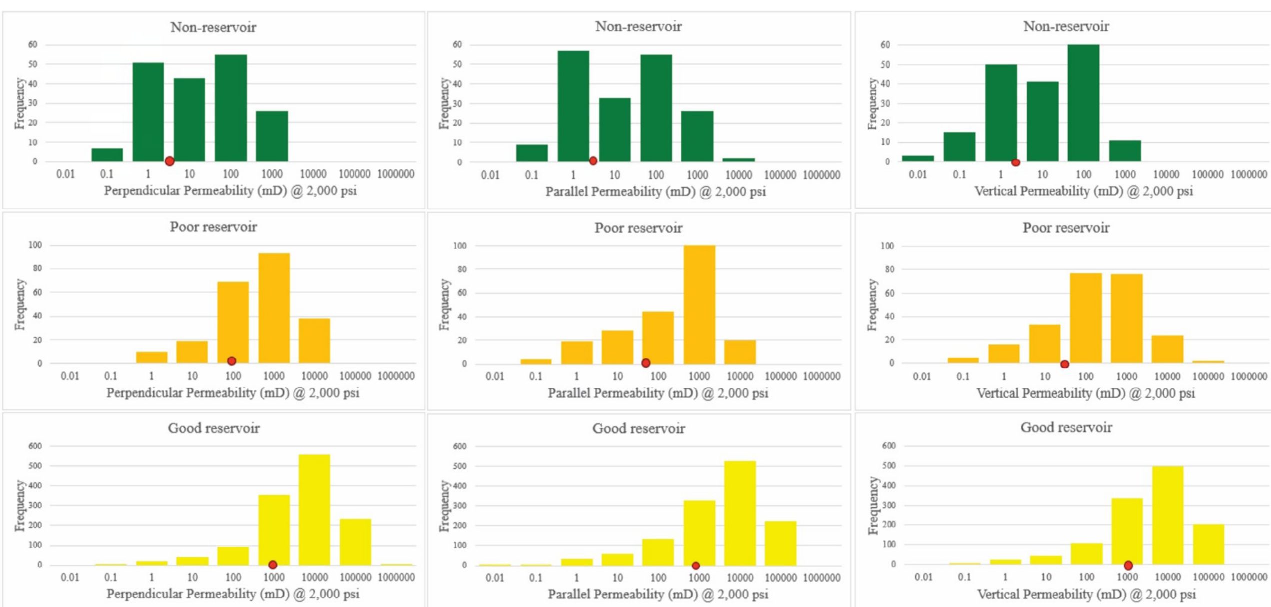

Figure 10 Frequency histogram for each permeability direction converted to confinement pressure at 2,000 psi, grouped by reservoir facies. The red dot represents the geometric mean for each reservoir facies.

Table 5 Geometric mean values of the permeabilities at 0 and 2,000 psi separated by lithology.

	Geometric mean of the permeability values (mD)					
	Perpendicular		Parallel		Vertical	
	0 psi	2,000 psi	0 psi	2,000 psi	0 psi	2,000 psi
Claystone	16	5	41	13	14	4
Siltstone	18	6	8	2	7	2
Fine Sandstone	336	118	183	63	142	48
Muddy Sandstone	533	190	526	187	597	214

Table 5 Cont.

	Geometric mean of the permeability values (mD)					
	Perpendicular		Parallel		Vertical	
Medium to coarse sandstone	2,377	891	1,693	627	1,994	743
Conglomerate	7,842	3,063	6,928	2,695	6,378	2,474
Intraformational Breccia	8,987	3,527	2,918	1,102	399	141

Green: Non-reservoir; Red: Poor reservoir; Yellow: Good reservoir

5 Conclusion

The goal of this study was to develop a method to make the permeability values collected in an outcrop compatible with confining pressure conditions equivalent to real reservoirs in the subsurface.

The results obtained produced a reliable equation for converting permeability values from the surface condition (@0 psi) to a usual confining pressure condition for important Maastrichtian reservoirs of the Brazilian Southeastern Margin (@2,000 psi). In addition, the application of this method to the database obtained for the Resende Formation outcrop studied in the Volta Redonda basin (RJ), with 5,000 in-situ permeability measurements, demonstrated how significant the reduction of permeability values can be in poorly consolidated sandstone reservoirs when they are under subsurface conditions. Furthermore, the permeability variation is enhanced by textural aspects and deformational structures (faults and deformation bands) present in the outcrop. This variation affects the fluid flow through a real reservoir, on which the previous knowledge is an important subsidy for planning production strategies.

The method proposed in this study can be applied in the oil industry and produce a new adjusted database. The results obtained show that it is possible to use the outcrop data in the same conditions of the analogous reservoir, and then apply the measurements in the geological model to fill the lack of information, reducing the uncertainty on these models and allowing better production management.

Based on the results achieved, a model analogous to poorly consolidated and tectonically deformed sandstone reservoirs will be built using the outcrop stratigraphical and structural characterization. This model will be filled with permeability data converted to depth conditions to carry out 3D flow simulations.

6 References

Andrade, T.P. 2020, 'Simulação sequencial gaussiana da distribuição espacial da permeabilidade em rochas siliciclásticas pouco consolidadas e fraturadas', Master Thesis, Universidade Federal do Rio de Janeiro.

Fiuza, B.O., Mello, C.L. & Ribeiro, C.S. 2020, 'Parâmetros de Densidade de Falhas e Bandas de Deformação em Rochas Siliciclásticas Pouco Consolidadas da Formação Resende, Eoceno, Bacia de Volta Redonda, Estado do Rio de Janeiro', *Geologia USP: Série Científica*, vol. 20, no. 4, pp. 39-52, DOI:10.11606/issn.2316-9095.v20-165065.

Galvão, M.S. 2018, 'O Papel das Falhas e Bandas de Deformação sobre o Fabric dos Arenitos da Formação Resende (Eoceno. *Rift* Continental do Sudeste do Brasil) e seu Impacto Sobre o Comportamento Hidromecânico', Master Thesis, Universidade Federal do Rio de Janeiro.

Howell, J.A., Martinius, A.W. & Good, T.R. 2014, 'The Application of Outcrop Analogues in Geologic Modelling: A Review, Present Status and Future Outlook', in A.W. Martinius, J.A. Howell & T.R. Good (eds), *Sediment-Body Geometry and Heterogeneity: Analogue Studies for Modelling the Subsurface.* Geologic Society Special Publications, Londres, vol. 387, pp. 1-25. DOI:10.1144/SP387.12.

Liao, Q.A. 2018, 'Fast Algorithm for the Estimation of the Equivalent Permeability in Heterogeneous Formations', *Paper presented at the Society of Petroleum Engineers - SPE Kingdom of Saudi Arabia Annual Technical Symposium and Exhibition 2018, Saudi Arabia*. DOI:10.2118/192295-MS.

Maciel, I.B., Mello, C.L. & Silva, A.T. 2017, 'Caracterização da deformação rúptil em afloramento da Formação Resende, Bacia de Volta Redonda, Estado do Rio de Janeiro', *Geologia USP: Série Científica,* vol. 17, no. 3, pp. 113-24, DOI:10.11606/issn.2316-9095.v17-391.

Mello, C.L., Barroso, E.V., Perosi, F.A., Ramos, R.R.C., Borges, A.F. & Polivanov, H. 2021, *Caracterização da deformação e de propriedades mecânicas e permoporosas* de arenitos pouco consolidados, Project Report, Universidade Federal do Rio de Janeiro.

Negrão, A.P., Ramos, R.R.C., Mello, C.L. & Sanson, M.S.R. 2015, 'Mapa Geológico do Cenozoico da Região da Bacia de Volta Redonda (RJ, Segmento Central do Rifte Continental do Sudeste do Brasil): Identificação de Novos Grabens e Ocorrências Descontínuas, e Caracterização de Estágios Tectonossedimentares', *Brazilian Journal of Geology*, vol. 45, no. 2, pp. 273-91, DOI:10.1590/23174889201500020007.

Negrão, A.P., Mello, C.L., Ramos, R.R.C., Sanson, M.S.R., Louro, V.H.A. & Bauli, P.G. 2020, 'Tectonosedimentary Evolution of the Resende and Volta Redonda Basins (Cenozoic, Central Segment of the Continental Rift of Southeastern Brazil)', *Journal of South American Earth Sciences*, vol. 104, 102789, DOI:10.1016/j.jsames.2020.102789.

Riccomini, C. 1989, ‘O *Rift* Continental do Sudeste do Brasil’, PhD Thesis, Universidade de São Paulo.

Riccomini, C., Sant'anna, L.G. & Ferrari, A.L. 2004, ‘A Evolução Geológica do Rift Continental do Sudeste do Brasil’, in V. Mantesso-Neto, A. Bartorelli, C.D.R. Carneiro & B.B. Brito-Neves *Geologia do Continente Sul-Americano: Evolução da Obra de Fernando Flávio Marques de Almeida*, Beca, pp. 383-405.

Sanson, M.S.R. 2006, ‘Sistemas Deposicionais Aluviais e Tectônica Rúptil na Região de Volta Redonda (RJ) - *Rift* Continental do Sudeste do Brasil’, Master Thesis, Universidade Federal do Rio de Janeiro.

Vogel, S.N. 2018, ‘Caracterização macroscópica e microscópica de aspectos texturais e estruturais relacionados à deformação rúptil de Arenitos Pouco Consolidados (Formação Resende, Bacia de Volta Redonda) e Aspectos Permoporosos Associados’, Master Thesis, Universidade Federal do Rio de Janeiro.

Author contributions

Camila Faria de Albuquerque: conceptualization; formal analysis; methodology; validation; writing-original draft; writing – review and editing; visualization. **Aline Theophilo da Silva:** validation; writing-original draft; writing – review and editing; supervision. **Claudio Limeira Mello:** validation; writing-original draft; writing – review and editing; supervision.

Conflict of interest

The authors declare no conflict of interest.

Data availability statement

Data available on request.

Funding information

Not applicable.

Editor-in-chief

Dr. Claudine Dereczynski

Associate Editor

Dr. Gerson Cardoso da Silva Jr.

How to cite:

Albuquerque, C.F., Silva, A.T. & Mello, C.L. 2024, ‘Permeability Data Treatment from Analogous Outcrop for Use in Three-Dimensional Reservoir Model’, *Anuário do Instituto de Geociências,* 47:59235. https://doi.org/10.11137/1982-3908_2024_47_59235